Journal of Visualized Experiments

An advanced murine model for nonalcoholic steatohepatitis in association with type 2 diabetes

--Manuscript Draft--

Article Type:	Invited Methods Article - JoVE Produced Video
Manuscript Number:	JoVE59470R1
Full Title:	An advanced murine model for nonalcoholic steatohepatitis in association with type 2 diabetes
Keywords:	Immunology and environmental exposure; obesity; Adaptive Immunology; insulin resistance; housing conditions; metabolic phenotyping; Flow Cytometry
Corresponding Author:	Julia Sbierski-Kind Charite Universitatsmedizin Berlin Berlin, GERMANY
Corresponding Author's Institution:	Charite Universitatsmedizin Berlin
Corresponding Author E-Mail:	julia.sbierski-kind@charite.de
Order of Authors:	Julia Sbierski-Kind
	Katharina Schmidt-Bleek
	Mathias Streitz
	Jonas Kath
	Joachim Spranger
	Hans-Dieter Volk
Additional Information:	
Question	**Response**
Please indicate whether this article will be Standard Access or Open Access.	Standard Access (US$2,400)
Please indicate the **city, state/province, and country** where this article will be **filmed**. Please do not use abbreviations.	Berlin, Berlin, Germany

Cover Letter

Dear Editors,

We would like to submit the enclosed manuscript entitled "An advanced murine model for nonalcoholic steatohepatitis in association with type 2 diabetes" for publication in *Jove.*

After the experimental discovery of the link between adipose tissue inflammation and the development of insulin resistance and following complications, the therapeutic potential of “interventional immunology” is a topic of interest. Despite successes in many different murine models, efficient translation to human intervention trials has been difficult. Laboratory mice kept in specific pathogen-free housing might not reflect relevant aspects of the antigen-experienced human immune system.

In the present manuscript, a simple and reliable diet-induced rodent animal model for nonalcoholic steatohepatitis is described, achieved through non-specific pathogen free housing of the animals and administration of a specific high-fat diet. We compared diet-induced obesity in SPF mice with those housed in non-SPF conditions being widely exposed to environmental germs and developing an “immune aged” phenotype. Here, we found that obesity-induced inflammation is profoundly affected by environmental conditions as antigen-experienced mice develop a distinct metabolic phenotype compared to mice maintained under SPF conditions.

Regarding the technical aspects of this manuscript, we provide a detailed protocol to identify hepatic and adipose immune cell subsets in an advanced mouse model to recapitulate human immunological conditions exposing mice to environmental germs.

We expect our findings not only to be of interest to experimental communities in the field of immunometabolism but also to reveal the limitations of specific pathogen free laboratory mice as immunological models. We hope that you will consider it favorably for publication in *Jove*. We affirm that the manuscript has been prepared in accordance with guidelines for authors. We have read the manuscript and the content of this manuscript has not been previously published in any journal, is not being submitted for publication elsewhere and has been approved by all authors. Finally, we confirm that we did not have any prior discussions with a *Jove* editor about the work described in the manuscript.

Sincerely, on behalf of all authors,

Julia Sbierski-Kind

Berlin November 30th, 2018

TITLE:

An Advanced Murine Model for Nonalcoholic Steatohepatitis in Association with Type 2 Diabetes

AUTHORS AND AFFILIATIONS:

Julia Sbierski-Kind[1,2,3,4], Katharina Schmidt-Bleek[3,6], Mathias Streitz[3,5], Jonas Kath[3,5], Joachim Spranger[1,2,4*], Hans-Dieter Volk[2,3,5*]

[1]Department of Endocrinology & Metabolism Charité - Universitätsmedizin Berlin, corporate member of Freie Universität Berlin, Humboldt-Universität zu Berlin, Berlin, Germany
[2]Berlin Institute of Health (BIH), Berlin, Germany
[3]Berlin-Brandenburg Center for Regenerative Therapies (BCRT), Charité - Universitätsmedizin Berlin, corporate member of Freie Universität Berlin, Humboldt-Universität zu Berlin, Berlin, Germany
[4]DZHK (German Centre for Cardiovascular Research), partner site Berlin, Germany
[5]Institute of Medical Immunology, Charité - Universitätsmedizin Berlin, corporate member of Freie Universität Berlin, Humboldt-Universität zu Berlin, Berlin, Germany
[6]Julius Wolff Institute (JWI) and Center for Musculoskeletal Surgery, Charité - Universitätsmedizin Berlin, Berlin, Germany, corporate member of Freie Universität Berlin, Humboldt-Universität zu Berlin, Berlin, Germany

*These senior authors contributed equally.

Corresponding Author:
Julia Sbierski-Kind
Julia.sbierski-kind@charite.de

Email Addresses of Co-authors:
Julia Sbierski-Kind (julia.sbierski-kind@charite.de)
Katharina Schmidt-Bleek (katharina.schmidt-bleek@charite.de)
Mathias Streitz (mathias.streitz@charite.de)
Jonas Kath (jonas.kath@charite.de)
Joachim Spranger (joachim.spranger@charite.de)
Hans-Dieter Volk (hans-dieter.volk@charite.de)

KEYWORDS:
Immunology and environmental exposure, obesity, adaptive immunology, insulin resistance, housing conditions, metabolic phenotyping, flow cytometry

SUMMARY:
A simple and reliable diet-induced rodent animal model for nonalcoholic steatohepatitis (NASH) is described, achieved through non-SPF housing of the animals and administration of a specific high-fat diet. We describe identification of hepatic and adipose immune cell subsets to recapitulate human immunological conditions by exposing mice to environmental germs.

ABSTRACT:

Obesity is associated with chronic low-grade inflammation and insulin resistance, contributing to an increasing prevalence of chronic metabolic diseases, such as type 2 diabetes and nonalcoholic steatohepatitis (NASH). Recent research has established that pro-inflammatory immune cells infiltrate obese hypertrophic adipose tissue and liver. Given the emerging importance of immune cells in the context of metabolic homeostasis, there is a critical need to quantify and characterize their modification during the development of type 2 diabetes and NASH. However, animal models that induce pathophysiological features typical of human NASH are sparse.

In this article, we provide a detailed protocol to identify immune cell subsets isolated from liver and adipose tissue in a reliable mouse model of NASH, established by housing high-fat diet (HFD) mice under non-specific pathogen-free (SPF) conditions without a barrier for at least seven weeks. We demonstrate the handling of mice in non-SPF conditions, digestion of the tissues and identification of macrophages, natural killer (NK) cells, dendritic cells, B and T cell subsets by flow cytometry. Representative flow cytometry plots from SPF HFD mice and non-SPF mice are provided. To obtain reliable and interpretable data, the use of antibodies, accurate and precise methods for tissue digestion and proper gating in flow cytometry experiments are critical elements.

The intervention to restore physiological antigen exposure in mice by housing them in non-SPF conditions and unspecific exposure to microbial antigens could provide a relevant tool for investigating the link between immunological alterations, diet-induced obesity and related long term complications.

INTRODUCTION:

Obesity is a multifactorial disorder and a major risk factor for developing heart disease, stroke, nonalcoholic steatohepatitis (NASH), type 2 diabetes (T2D) and some types of cancer. The prevalence of obesity is rapidly increasing globally. Today, 2.1 billion people – nearly 30% of the world's population – are either obese or overweight[1]. Obesity-associated insulin resistance can lead to T2D, when exhausted pancreatic islet beta cells fail to compensate for the increased need for insulin to maintain glucose homeostasis[2].

Adipose tissue is composed of various cell types including adipocytes, endothelial cells, fibroblasts and immune cells. During progression of obesity, changes in the number and activity of immune cells can lead to low-grade inflammation of hypertrophic adipose tissue[3,4]. Specifically, it has been found that excessive energy intake, accompanied by chronically elevated levels of blood glucose, triglycerides and free fatty acids, leads to adipocyte hypoxia, endoplasmic reticulum stress, impaired mitochondrial function and enhanced cytokine secretion, resulting in the activation of pro-inflammatory adipose immune cells[5,6]. Past research has mainly focused on innate immunity, but more recently adaptive immune cells (T and B cells) have emerged as important regulators of glucose homeostasis. They possess inflammatory (including $CD8^+$ T cells, Th1, and B cells) or primarily regulatory functions (including regulatory T (Treg) cells, Th2 cells) and can both exacerbate or protect against insulin resistance[7-9].

Furthermore, several mechanisms were proposed to explain how obesity increases steatohepatitis, including increased production of cytokines by adipose tissue[10]. NASH, the progressive form of nonalcoholic fatty liver disease and a major health burden in developed countries, is histologically characterized by ballooned hepatocytes, lipid accumulation, fibrosis and pericellular inflammation and may progress to cirrhosis, end stage liver disease or hepatocellular carcinoma. Several regimen (for instance the methionine and choline deficient diet[11]) are known to induce NASH-like liver pathology in non-human animal models, but most of these approaches do not recapitulate human conditions of NASH and its metabolic consequences as they either require specific gene knockout, non-physiological dietary manipulations or lack insulin resistance typical of human NASH. Moreover, our understanding of the underlying mechanisms of metabolic diseases is currently based on experiments carried out with laboratory mice housed under standard specific pathogen free (SPF) conditions. Those barrier facilities are abnormally hygienic and do not consider the microbial diversity humans have to encounter, which may account for difficulties in the translation process of animal studies to clinical approaches[12-14].

To investigate the different immune cell subsets in adipose tissue and liver during the development of insulin resistance and NASH in an advanced mouse model reproducing human immunological conditions, mice were housed in individual cages in semi sterile conditions without a barrier. Mice housed under antigen exposed conditions developed NASH-like liver pathology already after 15 weeks of high-fat diet (HFD) feeding[13]. Compared to age-matched SPF mice they developed macrovesicular steatosis, hepatic infiltration and activation of immune cells. This manuscript describes a robust flow cytometry analysis to define and count immune cell subsets from mouse adipose tissue and liver in a model of NASH. Flow cytometry analysis allows the detection of multiple parameters of individual cells simultaneously in contrast to RT-PCR or immunohistochemistry approaches.

In summary, our study offers a mouse model of short-term HFD for investigating the development of insulin resistance and NASH and the underlying mechanisms that also exhibits fidelity to the human condition.

PROTOCOL:

This study was carried out in accordance with the Guide for the Care and Use of Laboratory Animals of the National Institutes of Health and the Animal Welfare Act under the supervision of our institutional Animal Care and Use Committee. Animal protocols were conducted according to institutional ethical guidelines of the Charité Berlin, Germany, and were approved by the Landesamt für Gesundheit und Soziales and comply with the ARRIVE guidelines.

1. Diet-induced animal model of steatohepatitis

1.1) Transfer mice (C57Bl/6J, male) to non-SPF housing at the age of 4 weeks and expose them continuously to a broad range of environmental pathogens/antigens. Guarantee the exposure by daily handling of the laboratory animals as antigens are distributed by air passage in this way.

1.2) Maintain mice (W57Bl/6J, male, 12 weeks old) in open caging systems with conventional filters on a 12 h:12 h light/dark cycle at a temperature of 22 °C. Do not irradiate or autoclave experimental diet and bedding. Access animal housing facility without mask or hairnet. Open roors between animal rooms. Do not use an airshower.

1.3) Guarantee daily handling of the laboratory animals and switch rooms on a regular basis so that antigens are distributed by air passage. Complement dirty housing with daily non-specific microbial exposure to antigens from bedding of mammalian laboratory animals housed in rooms next to the laboratory mice.

1.4) Measure proportions of $CD44^{-}CD62L^{-}$ effector memory $CD4^{+}$ and $CD8^{+}$ T cells in blood and spleen using flow cytometry as described in Ref.[13].

NOTE: In this regard we defined an increase of 20% of effector memory $CD8^{+}$ T cells from $CD8^{+}$ T cells as evidence of sufficient microbial exposure.

1.5) Start HFD (60 kJ% from fat, 19 kJ% from proteins and 21 kJ% from carbohydrates and ad libitum consumption of water with 6% sucrose content with five-week old C57Bl/6J male mice for seven weeks. The HFD should contain 60% kJ from fat (as described above) in order to induce the development of insulin resistance throughout the course of the experiment.

NOTE: Hematoxylin staining should be performed and histological characteristics as hepatocyte ballooning, Mallory Denk bodies, immune cell infiltration and macrovesicular steatosis must be found to demonstrate NASH-like liver pathology as shown in Ref.[13].

2. Preparation of reagents and solutions

2.1) Prepare 70% ethanol, phosphate buffered saline (PBS, without calcium and magnesium) supplemented with 0.5% BSA and ACK (Ammonium-Chloride-Potassium) lysis buffer.

2.2) Staining buffer

2.2.1) Dissolve 10 mL of fetal calf serum (FCS) in 500 mL of PBS to obtain 2% FCS PBS. Place staining buffer on ice before use.

2.2.2) Store solution in a plastic bottle at 4 °C.

2.3) Collagenase solution for adipose tissue digestion

2.3.1) Dissolve 2.5 g of bovine serum albumin (BSA) in 500 mL of PBS to obtain a 0.5% BSA/PBS.

2.3.2) Dissolve 74.5 g of $CaCl_2$ in 10 mL of 0.5% BSA/PBS to obtain a 10 mM $CaCl_2$ solution.

2.3.3) Add 1 mg of collagenase type II (see **Table of Materials**) to each mL of 0.5% BSA with 10 mM $CaCl_2$ PBS.

2.3.4) Prepare 3 mL of collagenase digest solution per g of adipose tissue sample. Prepare fresh collagenase solution for each isolation.

2.4) Collagenase solution for liver tissue digestion

2.4.1) Dissolve 2.5 g of BSA in 500 mL of Hank´s Balanced Salt Solution (HBSS) to obtain 0.5% BSA HBSS.

2.4.2) Add 10 mL of FCS in 500 mL of 0.5% BSA/PBS to obtain 2% FCS 0.5% BSA/PBS.

2.4.3) Add 0.5 mg of collagenase type IV (see **Table of Materials**) to each mL of 2% FCS 0.5% BSA/PBS.

2.4.4) Add 0.02 mg of DNase per mL of 2% FCS 0.5% BSA/PBS collagenase solution.

2.4.5) Prepare 13 mL of collagenase digest solution per liver tissue sample.

2.4.6) Prepare fresh collagenase solution for each isolation.

3. Generation of single cell suspensions

3.1) Adipose tissue digestion

3.1.1) Euthanize mice via isoflurane anesthesia followed by cervical dislocation. Spray the chest with 70% ethanol. Carefully make a 5-6 cm central incision through the integument and abdominal wall along the entire length of the rib cage to expose the pleural cavity and heart.

NOTE: Do not damage underlying organs and keep scissors tips up.

3.1.2) Inject at least 10 mL of 0.9% saline solution in the apex of the left ventricle using a 26 G needle.

NOTE: Successful perfusion is noted by blanching of the liver.

3.1.3) Open the peritoneal cavity with scissors and cut out the perigonadal fat pads on each side with fine curved scissors. Dissect gonadal tissues with fine curved scissors and weigh adipose tissue.

3.1.4) Perform the mechanical dissociation using scissors and cut adipose tissue into fine pieces in a Petri dish at 4 °C. Transfer adipose tissue to 50 mL conical centrifuge tubes and rinse Petri dish with 1 mL of 0.5% BSA/PBS.

3.1.5) Add 3 mL of adipose tissue digest solution (as prepared in step 2.3) per gram of adipose tissue. Incubate adipose tissue solution at 37 °C for 20 min under gentle shaking (200 rpm).

3.1.6) Add 5 mL of 0.5% BSA/PBS per gram of adipose tissue and place on ice. Triturate the solution numerous times with a 10 mL serological pipette and pass it through a strainer (100 µm) with the aid of a plunger.

3.1.7) Centrifuge at 500 x *g* for 10 min at 4 °C.

3.1.8) Remove the floating adipocyte fraction by pipetting. Resuspend the cell pellet (stromal vascular fraction) in 1 mL of ACK lysis buffer (see **Table of Materials**). Add 10 mL of 2% FCS PBS.

3.1.9) Centrifuge at 500 x *g* for 10 min at 4 °C.

3.1.10) Decant supernatant and resuspend cell pellet in 250 µL of 2% FCS PBS.

3.1.11) Count the number of viable cells on a hemocytometer using Trypan blue exclusion.

3.2) Liver tissue digestion

3.2.1) Store liver in a conical centrifuge tube filled with PBS and transport on ice.

3.2.2) Perform the mechanical dissociation using syringe stamps in a Petri dish at 4 °C. Put dissected liver tissue in a 50 mL conical centrifuge tube containing 10 mL of warm liver digest solution. Rinse the Petri dish with 3 mL of liver digest solution.

3.2.3) Incubate liver tissue solution at 37 °C for 20 min under gentle shaking (200 rpm).

3.2.4) Add 20 mL of HBSS. Triturate the solution numerous times with a 10 mL serological pipette and pass it through a strainer (100 µm) with the aid of a plunger.

3.2.5) Centrifuge at 500 x *g* for 10 min at 4 °C. Decant the supernatant and resuspend the cell pellet in 20 mL of HBSS.

3.2.6) Centrifuge at 30 x g for 1 min at room temperature to remove the hepatocyte matrix. Discard the cell pellet.

3.2.7) Centrifuge the supernatant at 500 x *g* for 10 min at 4 °C. Resuspend the pellet in 10 mL of 33% low viscosity density gradient medium solution (see **Table of Materials**) in HBSS followed by centrifugation (800 x *g*; 30 min; room temperature; no brake).

3.2.8) Resuspend the pellet in 1 mL of ACK lysis buffer and incubate for 4 min at room temperature. Then add 10 mL of HBSS.

NOTE: To discard the supernatant aspirate the supernatant with interphase (hepatocytes) very carefully with a transfer pipette (as much as possible without taking the pellet with immune cells and erythrocytes).

3.2.9) Pass cells through a 30 µm strainer in 15 mL conical centrifuge tube and centrifuge 500 x *g* for 10 min at 4 °C. Decant supernatant and resuspend cell pellet in 250 µL of 2% FCS PBS.

3.2.10) Count the number of viable cells on a hemocytometer using Trypan blue exclusion.

4. Surface staining

4.1) Prepare antibody mix for T-cell-subsets (Panel 1) and innate immune cells (Panel 2) as described in **Table 1** and **Table 2**. Volumes are optimized for one sample (100 µL) regarding to antibody concentrations.

NOTE: Lymphocytes and innate immune cells present differences in autofluorescence and should be analyzed separately.

4.2) Use up to 3 x 10^6 cells in 100 µL in a polystyrene FACS tube for surface staining. To block Fc receptors add 10 µL of anti-CD16/CD32 antibody (diluted 1:100) and incubate for 10 min on ice. Use an unstained negative control sample to adjust side scatter (SSC) and forward scatter (FSC) to determine the location of the negative cell population.

4.3) Vortex and add the appropriate volume of antibody mixture for Panel 1 and Panel 2. Add 1 µL of viability dye to each sample to allow for live and dead cell discrimination. Incubate for 20 min at 4 °C and protected from light.

4.4) Wash two times with 2 mL of 2% FCS PBS and centrifuge at 300 x *g* for 5 min at 4 °C.

4.5) Resuspend the cell pellet in 300 µL of 2% FCS PBS and store at 4 °C until FACS analysis.

NOTE: Before starting the measurement pass cells through 30 µm cell strainer into polystyrene FACS tube and vortex. Flow cytometry was performed with labeled cells stored in 2% FCS PBS at 4 °C for 1-3 hours. Cells should be analyzed as soon as possible for optimized results.

5. Flow cytometry compensation, acquisition and gating

5.1) Run unstained negative control sample to set the FSC and SSC and adjust voltages of the flow cytometer to detect leucocyte populations and to distinguish between debris and viable cells. Exclude debris and dead cells.

NOTE: Viability of the cell suspensions from the liver might be lower than the viability from the cell suspensions from perigonadal adipose tissue due to an additional density separation step.

5.2) Run single stained control samples for multi-color compensation.

NOTE: Antibody capture beads could also be used to adjust for spectral overlap if the number of cells of a cell population of interest is too low to compensate using cells. To detect possible autofluorescence signals of the cells fluorescence minus one (FMO) controls for every antibody are recommended but were not applied in this protocol.

5.3) Start the measurement, collect appropriate number of events (at least 50,000 events) and record experimental data.

5.4) Export FCS data files for analysis and set the gating strategy. Gate on $CD45^+$ leucocytes to identify subsequent cell populations.

REPRESENTATIVE RESULTS:

The protocol described allows the characterization of surface markers of innate and adaptive immune cells isolated from murine perigonadal adipose tissue and liver in a model of diet-induced NASH. In this model, NASH was induced by administration of HFD plus sucrose (6%) in drinking water for 7 to 15 weeks in C57Bl/6J mice, as previously reported[13]. Importantly, mice were housed in semi sterile conditions and, thus, exposed to environmental antigens throughout the experiment. HFD fed mice housed in SPF conditions and chow diet mice housed under SPF and non-SPF conditions served as controls. HFD feeding resulted in significant body weight gain already after 7 weeks in both groups. A significant difference in body weight was first evident at week 4 ($P < 0.001$) and remained significant throughout the following experimental weeks. However, no significant differences in weight gain were shown between SPF and non-SPF mice after 7 weeks[13]. The stromal vascular fraction and immune cells from perigonadal adipose tissue and livers of male mice fed a HFD for 7 weeks were isolated by collagenase digestion. Immune cells were labeled with fluorophore-conjugated primary antibodies and proportions of T cells, B cells, macrophages, NK cells, dendritic cells and granulocytes were quantified via flow cytometry analysis. Gating for T cell subpopulations, including doublet discrimination, and viability staining, in murine perigonadal fat is illustrated in **Figure 1**. $CD45^+$ leucocytes are first gated for CD4 and CD8 and subsequently gated for CD44 and CD62L to discriminate between naïve, central memory, effector memory and effector T cells. $CD44^+$ cells were then further characterized with CD127, KLRG1 and PD-1. **Figure 2** provides the gating strategy for analyzing B cells, granulocytes, NK cells, macrophages and dendritic cells.

Representative results of extracellular staining of T cells within murine liver of HFD exposed mice compared to HFD SPF mice are demonstrated in **Figure 3A**. Indeed, a higher percentage of effector memory $CD4^+$ and $CD8^+$ T cells can be detected in HFD exposed mice, whereas intrahepatic naïve $CD4^+$ and $CD8^+$ T cells were found to be considerably lower in exposed compared to SPF mice at week 7 (**Figure 3A**).

To validate these results, the hepatic inflammatory response associated with antigen exposure was investigated by hematoxylin/eosin staining of liver sections of 15 weeks fed mice[13]. Severe steatosis, including increase of large lipid droplets resulting in macrovesicular steatosis, lobular inflammation, hepatocellular ballooning and destroyed lobular structure, was found in HFD exposed mice while only some SPF mice displayed a mild fat accumulation in the liver (**Figure 3B**). As reported in **Figure 3C**, the percentage of NK cells was higher in perigonadal adipose tissue of HFD exposed mice, whereas HFD SPF mice showed higher percentages of dendritic cells. No significant differences were found for macrophages and monocytes. Altogether, these results confirm more severe hepatic steatosis in HFD exposed mice and minor differences in adipose tissue between HFD exposed and SPF mice.

Table 1 shows the antibodies used in panel 1. Antibodies used in flow cytometry analysis for extracecullar staining of B cells, macrophages, NK cells, dendritic cells and granulocytes are depicted in **Table 2**.

FIGURE AND TABLE LEGENDS:

Figure 1: Schematic representation of gating strategy used in flow cytometry analysis of adipose immune cells (panel 1). First debris is excluded by using forward scatter area (FSC-A) and side scatter area (SSC-A) and choosing the correct size. The cells are then gated on singlets and are further characterized by the expression of CD45. Viable cells are selected using alive/dead cell marker that is an amine reactive fluorescent dye that is non-permeant to live cells, but permeant to the cells with compromised membranes. T cells were divided into cytotoxic T cells ($CD8^+$) and T-helper cells ($CD4^+$) and subdivided into naïve ($CD44^+CD62L^-$), central memory ($CD44^+CD62L^+$), effector memory ($CD44^+CD62L^-$) and effector ($CD44^-CD62L^+$) T cells. Finally, $CD44^+$ cells are gated on KLRG1, CD127 and PD-1.

Figure 2: Schematic representation of gating strategy used in flow cytometry analysis of adipose immune cells (panel 2). Gating of dendritic cells was based on CD11b and CD11c expression. The following other populations were defined: B cells, NK cells, macrophages, monocytes and granulocytes. Data were analyzed after acquisition with the appropriate software.

Figure 3: Representative flow cytometry analysis of T cells isolated from murine perigonadal adipose tissue and liver. A) $CD4^+$ and $CD8^+$ T cells of murine livers from 7week HFD mice maintained under SPF and exposed conditions were analyzed *via* flow cytometry. **B)** Representative staining of 15 week HFD SPF and exposed mice. Infiltration of immune cells and ballooned hepatocytes (arrowhead) illustrate NASH. **C.** Percentages of adipose innate immune cells as percentage of leukocytes in HFD mice maintained under SPF or exposed conditions for 7 weeks. n=6-10 mice per group. Significance was determined using two-way ANOVA multiple measurement. Data are represented as mean ± SEM. ** $P < 0.01$, *** $P < 0.001$. This figure has been modified from[13].

Table 1: Antibodies used in flow cytometry for extracellular staining (Panel 1). The amount of antibody described is for the analysis of one sample.

Table 2: Antibodies used in flow cytometry for extracellular staining (Panel 2). The amount of antibody described is for the analysis of one sample.

DISCUSSION:

Steatohepatitis has a strong association with metabolic abnormalities such as obesity, insulin resistance and dyslipidemia[15]. Multiple studies indicate that adipose tissue inflammation can drive the pathogenesis of type 2 diabetes, including altered levels of cells of both the innate and adaptive immune system[4,5,16,17]. In addition, it has been found that obesity modulates the activation of immune pathways, which can lead to liver complications[18]. There is an increasing interest in the characterization of immune cell phenotypes in adipose and liver inflammatory response because each immune cell subpopulation contributes in a different way to the development of insulin resistance and steatohepatitis.

This method gives detailed information about how to isolate and quantify relative amounts of immune cells from perigonadal adipose tissue and liver. Furthermore, the methods show how to maintain HFD fed mice in non-SPF conditions in order to induce steatohepatitis. The protocol can be used to study immune cell functions and to investigate associations of specific immune cells between different tissues in a microbiologically normalized environment.

In our present study, HFD feeding of non-SPF mice resulted in the development of insulin resistance and steatohepatitis, whereas HFD SPF mice developed insulin resistance, mild hepatic steatosis, but not steatohepatitis as determined by immunohistochemistry. Moreover, adipose and liver immune cell subsets differed significantly between HFD exposed and SPF mice, which confirms our understanding of the significance of different housing conditions. In summary, we could show that microbial exposure to commensal flora could influence the immunological properties of C57Bl/6 mice dramatically. Previous work has shown that the diversity and function of the gut microbiome is affected by diet-induced obesity[19,20] and that gut barrier function and intestinal permeability depend on housing conditions[21]. We aim to address the link between gut colonization and adipose and liver inflammation in an upcoming publication.

Several points have to be considered during the planning stage of the proposed methods. First, single-cell suspensions are required for all flow cytometry assays and cell viability may be affected by the level of mechanical tissue dissociation and the duration of enzymatic tissue digestion. In order to avoid the destruction of the antibody epitope and to maximize the yield of functionally viable, dissociated cells, the type of tissue, age of the animal, genetic modifications, concentrations of enzymes, temperature and incubation times should be taken into consideration.

Second, our protocol has been optimized to quantitatively determine different immune cell phenotypes from obese HFD fed mice with adipose tissue inflammation and steatohepatitis. As tissue integrity, the number of immune cells and, thus, the quality of tissue digestion, might be

affected by inflammatory processes, the protocol and collagenase used should be optimized for other tissues than liver or adipose tissue in specific experiments relating to dissection methods, incubations times or the collagenase used to digest the tissue. Third, it is important for the protocol that different experimental groups are included each day to eliminate effects due to day-to-day variation of the flow cytometry assay (temperature, incubation times, etc.).

However, there are some important limitations of the described method. In order to discriminate positive versus negative signals to properly adjust the gates to identify the cells positive for specific surface markers in the experimental samples, Fluorescence Minus One (FMO) controls (an FMO control contains all the fluorochromes in a panel, except for the one that is being measured) should have been used. In this experiment the data could be properly compensated and the gating was clear, but we recommend to add FMO controls to the experimental setup, whenever possible. Moreover, FoxP3, which needs to be stained intracellularly requiring permeabilization of the cell membrane, should have been used to quantify regulatory T cells because it allows a more accurate definition than the use of CD25 and CD127 (**Table 2**). Even though flow cytometry allows the quantification of several surface markers simultaneously, their number is limited to 12 per sample due to overlap in emission spectra. To correct for spectral overlap, time-intensive fluorescence compensation is required. To account for this, strategic panel development or the use of mass cytometry techniques is required. Furthermore, difficulties could arise in housing the mice in non-SPF conditions with regard to specific animal housing guidelines, but the current small number of studies on non-SPF rodents shows that such studies are possible[12,21]. For example, separated animal facilities for SPF and non-SPF mice could be evaluated. The development of a human adult-like immune system is compromised in SPF mice[12,21], resulting in limitations to translate treatment strategies from animal experiments to clinical studies.

In conclusion, we provide a detailed protocol for phenotypic characterization of murine adipose and hepatic immune cells using flow cytometry in a diet-induced animal model of NASH and insulin resistance. Considering the complex function and regulation of both innate and adaptive cells in the context of obesity and metabolic dysregulation, our proposed methods should help to deepen our understanding of immunological mechanisms to balance metabolic homeostasis and, thus, help to develop human therapeutics that can restore anti-inflammatory immune responses. Overall, the provided animal model serves as a rapid and robust model for assessing metabolic complications associated with obesity and can be applied to other disease models.

ACKNOWLEDGMENTS:

We thank Anke Jurisch, Diana Woellner, Dr. Kathrin Witte and Cornelia Heckmann for assistance with experimental procedures and Benjamin Tiburzy from Biolegend for helpful comments on the gating strategy. J.S. was supported by the Helmholtz Grant (ICEMED). This study was supported by grants from the Clinical Research Unit of the Berlin Institute of Health (BIH), the "BCRT-grant" by the German Federal Ministry of Education and Research and the Einstein Foundation. K.S.-B. and H.-D.V. are funded by FOR2165.

DISCLOSURES:

The authors have nothing to disclose.

REFERENCES:

1 Guh, D. P. et al. The incidence of co-morbidities related to obesity and overweight: A systematic review and meta-analysis. *BMC Public Health.* **9**, 88 (2009).

2 Prentki, M. Islet β cell failure in type 2 diabetes. **116** (7), 1802-1812 (2006).

3 Shoelson, S. E., Lee, J., Goldfine, A. B. Inflammation and insulin resistance. *Journal of Clinical Investigation.* **116** (7), 1793-1801 (2006).

4 Kahn, S. E., Hull, R. L., Utzschneider, K. M. Mechanisms linking obesity to insulin resistance and type 2 diabetes. *Nature.* **444** 840 (2006).

5 Exley, M. A., Hand, L., O'Shea, D., Lynch, L. Interplay between the immune system and adipose tissue in obesity. *Journal of Endocrinology.* **223** (2), R41-R48 (2014).

6 Ferrante, A. W. Macrophages, fat, and the emergence of immunometabolism. *Journal of Clinical Investigation.* **123** (12), 4992-4993 (2013).

7 Winer, D. A. et al. B cells promote insulin resistance through modulation of T cells and production of pathogenic IgG antibodies. *Nature Medicine.* **17** 610 (2011).

8 Onodera, T. et al. Adipose tissue macrophages induce PPARγ-high FOXP3(+) regulatory T cells. *Scientific Reports.* **5** (2015).

9 Lackey, D. E., Olefsky, J. M. Regulation of metabolism by the innate immune system. *Nature Reviews Endocrinology.* **12** 15 (2015).

10 Calle, E. E., Kaaks, R. Overweight, obesity and cancer: epidemiological evidence and proposed mechanisms. *Nature Reviews Cancer.* **4** 579 (2004).

11 Ibrahim, S. H., Hirsova, P., Malhi, H., Gores, G. J. Animal Models of Nonalcoholic Steatohepatitis: Eat, Delete, and Inflame. *Digestive Diseases and Sciences.* **61** (5), 1325-1336 (2016).

12 Beura, L. K. et al. Recapitulating adult human immune traits in laboratory mice by normalizing environment. *Nature.* **532** (7600), 512-516 (2016).

13 Sbierski-Kind, J. et al. Distinct Housing Conditions Reveal a Major Impact of Adaptive Immunity on the Course of Obesity-Induced Type 2 Diabetes. *Frontiers in Immunology.* **9** (1069) (2018).

14 Japp, A. S. et al. Wild immunology assessed by multidimensional mass cytometry. *Cytometry Part A.* **91** (1), 85-95 (2017).

15 Benedict, M., Zhang, X. Non-alcoholic fatty liver disease: An expanded review. *World Journal of Hepatology.* **9** (16), 715-732 (2017).

16 McNelis, Joanne C., Olefsky, Jerrold M. Macrophages, Immunity, and Metabolic Disease. *Immunity.* **41** (1), 36-48.

17 Ferrante, A. W. The Immune Cells in Adipose Tissue. *Diabetes, Obesity & Metabolism.* **15** (0 3), 34-38 (2013).

18 Bertola, A. et al. Hepatic expression patterns of inflammatory and immune response genes associated with obesity and NASH in morbidly obese patients. *PloS One.* **5** (10), e13577 (2010).

19 Turnbaugh, P. J., Bäckhed, F., Fulton, L., Gordon, J. I. Diet-Induced Obesity Is Linked to Marked but Reversible Alterations in the Mouse Distal Gut Microbiome. *Cell Host & Microbe.* **3** (4), 213-223.

20 Singh, R. K. et al. Influence of diet on the gut microbiome and implications for human health. *Journal of Translational Medicine.* **15** (1), 73 (2017).

21 Müller, V. M. et al. Gut barrier impairment by high-fat diet in mice depends on housing conditions. *Molecular Nutrition & Food Research.* **60** (4), 897-908 (2016).

Figure1

Click here to access/download;Figure;Figure 1.pdf

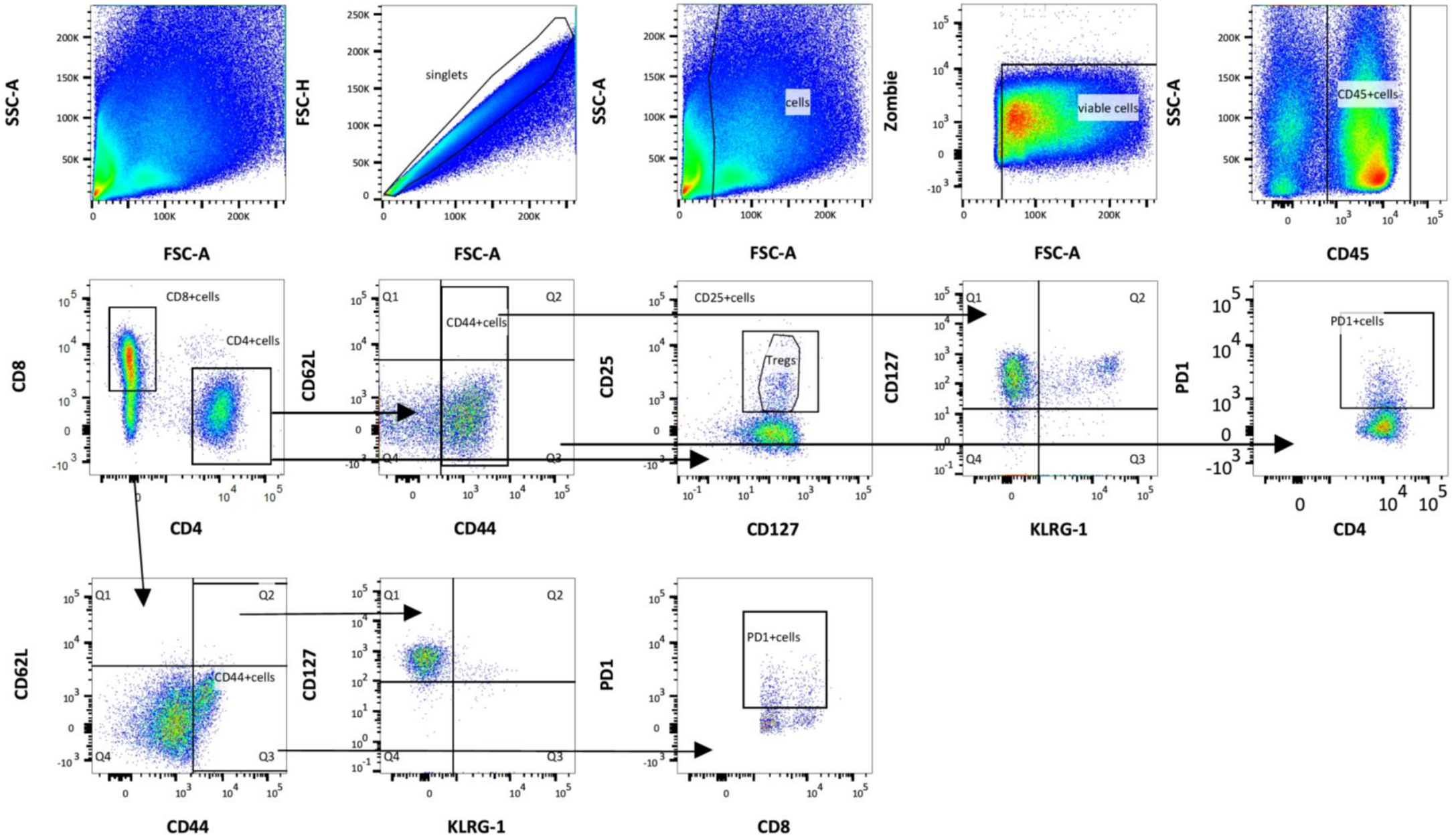

Figure2

Click here to access/download;Figure;Figure 2.pdf

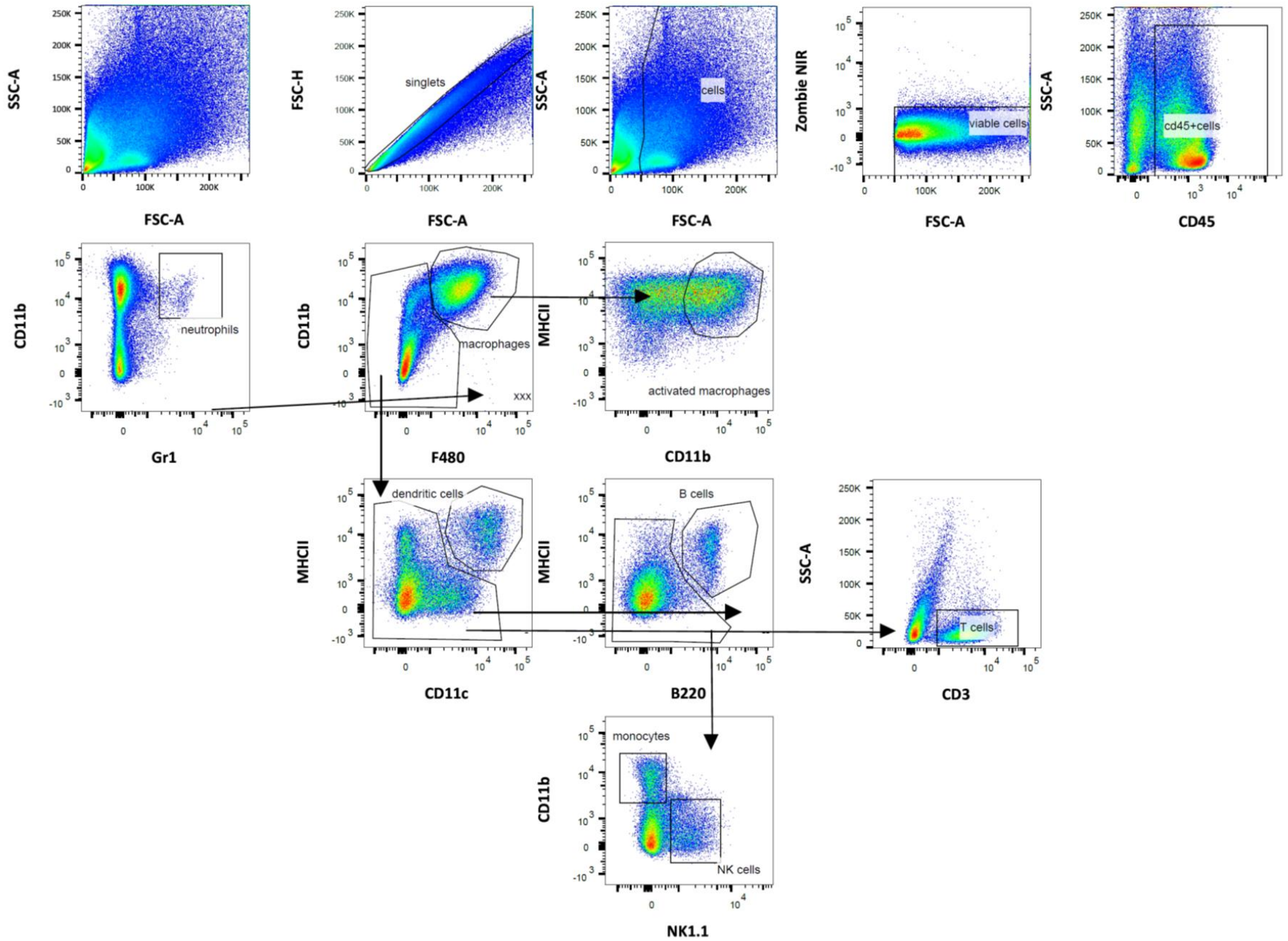

Figure3

Click here to access/download;Figure;Figure 3.pdf

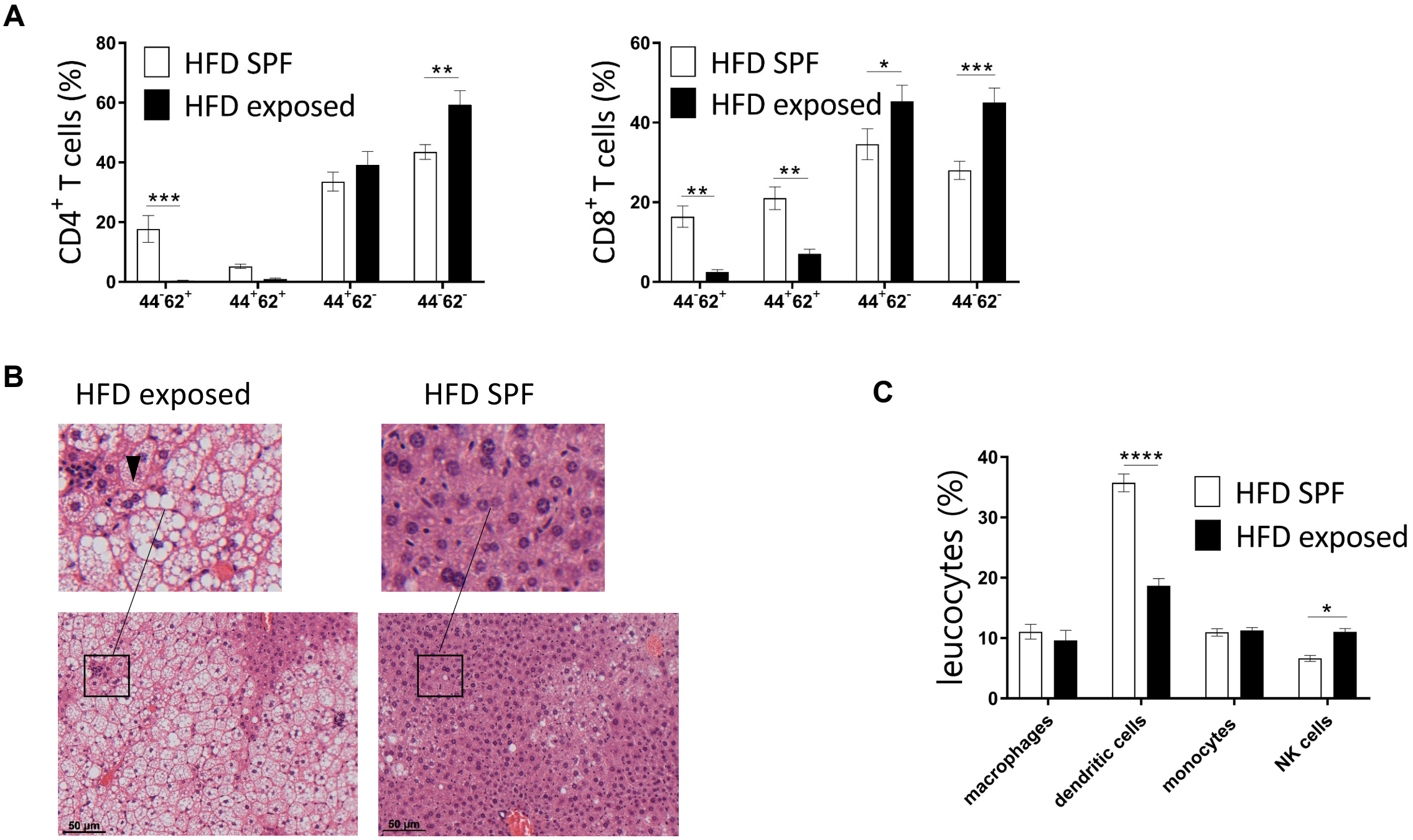

Table1

Laser (nm)	Filters	Fluorochrome	Surface Marker	Dilution	Volume for master mix solution (µl)
488 nm	blue 525/50	FITC	CD3	1:250	0.4
	blue 695/40	PerCp-Cy5.5	CD44	1:200	0.5
561 nm	gy 585/15	PE	CD25	1:200	0.5
	gy 610/10	PE-Dazzle	CD4	1:1000	0.1
	yg 670/30				
	yg 710/50				
	yg 780/60	PE/CY7	CD62L	1:200	0.5
638 nm	red 670/14	APC	KLRG-1	1:333	0.3
	red 710/50	A700	CD45	1:400	0.25
	red 780/60	NIR	Zombie	1:200	0.5
405 nm	violet 450/50	BV421	CD127	1:143	0.7
	violet 525/50				
	violet 610/20	BV605	CD279 (PD-1)	1:143	0.7
	violet 660/20				
	violet 710/50				
	violet 780/60	BV785	CD8a	1:333	0.3

Table2

Laser (nm)	Filters	Fluorochrome	Surface Mark	Dilution	Volume for master mix solution (µl)
488 nm	blue 525/50	**FITC**	**CD3**	**1:250**	**0.4**
	blue 695/40	**PerCp-Cy5.5**	**Gr1**	**1:125**	**0.8**
561 nm	gy 585/15	**PE**	**Siglec-F**		
	gy 610/10	**PE-Dazzle**	**CD4**	**1:1000**	**0.1**
	yg 670/30				
	yg 710/50				
	yg 780/60	**PE/CY7**	**MHCII**	**1:2000**	**0.05**
638 nm	red 670/14	**APC**	**CD11c**	**1:167**	**0.6**
	red 710/50	**A700**	**CD45**	**1:400**	**0.25**
	red 780/60	**NIR**	**Zombie**	**1:200**	**0.5**
405 nm	violet 450/50	**BV421**	**F4/80**	**1:100**	**1**
	violet 525/50				
	violet 610/20	**BV605**	**NK1.1**	**1:143**	**0.7**
	violet 660/20	**BV650**	**CD11b**	**1:100**	**1**
	violet 710/50	**BV710**	**B220**	**1:333**	**0.3**
	violet 780/60	**BV785**	**CD8a**	**1:333**	**0.3**

Table of Materials

Click here to access/download;Table of Materials;JoVE_Materials.xls

Name of Material/ Equipment	Company	Catalog Number
100µm cell strainers	Falcon	352340
1ml syringe	BD	309659
26G x 5/8 needles	BD	305115
35mm Petri Dishes	Falcon	353001
40µm cell strainers	Falcon	352340
ACK lysis buffer	GIBCO	A1049201
Alexa Fluor 700 anti-mouse CD45	Biolegend	103127
Analysis software	FlowJo 10.0.8 software	
APC anti-mouse CD11c Antibody	Biolegend	117309
APC anti-mouse KLRG1 (MAFA) Antibody	Biolegend	138411
BV421 anti-mouse CD127 Antibody	Biolegend	135023
BV421 anti-mouse F4/80 Antibody	Biolegend	123131
BV605 anti-mouse CD279 (PD-1) Antibody	Biolegend	135219
BV605 anti-mouse NK-1.1 Antibody	Biolegend	108739
BV650 anti-mouse/human CD11b Antibody	Biolegend	101239
BV711 anti-mouse/human B220 Antibody	Biolegend	103255
BV785 anti-mouse CD8a Antibody	Biolegend	100749
C57Bl/6J mice, male, 5 weeks old	Forschungseinrichtungen für experimentelle Medizin (**FEM**)	
CaCl2	Charité - Universitätsmedizin Ber	A119.1
Collagenase NB 4G Proved Grade	SERVA	11427513
Collagenase Typ I	Worthington	LS004197
Conical centrifuge tube 15ml	Falcon	352096
Conical centrifuge tube 50ml	Falcon	352070
DNAse	Sigma-Aldrich	4716728001
Fetal bovine serum	Biochrom	S0115
Filter 30µm	Celltrics	400422316
FITC anti-mouse CD3 Antibody	Biolegend	100203
Flow cytometry	BD-LSR Fortessa	
Forceps	Sigma-Aldrich	F4142-1EA
HBSS	Bioanalytic GmBH	085021-0500

High-fat diet	SSNIF	E15741–34
micro dissecting scissors	Sigma-Aldrich	S3146
PE anti-mouse CD25 Antibody	Biolegend	101903
PE/Cy7 anti-mouse CD62L Antibody	Biolegend	104417
PE/Cy7 anti-mouse I-A/I-E (MHCII) Antibody	Biolegend	107629
PE/Dazzle 594 anti-mouse CD4 Antibody	Biolegend	100565
Percoll solution	Biochrom	L6115
PerCP/Cy5.5 anti-mouse CD44 Antibody	Biolegend	103031
PerCP/Cy5.5 anti-mouse Gr-1 Antibody	Biolegend	108427
Phosphate buffered saline	Gibco	12559069
Round-Bottom Tubes with cell strainer cap	STEMCELL Technologies	38030
TruStain fcX anti-mouse CD16/32	Biolegend	101301
Trypan Blue	Sigma-Aldrich	T6146
Zombie NIR Fixable Viability Kit	Biolegend	423105

Comments/Description

AB_493714 (BioLegend Cat. No. 103127)

AB_313778 (BioLegend Cat. No. 117309)
AB_10645509 (BioLegend Cat. No. 138411)
AB_10897948 (BioLegend Cat. No. 135023)
AB_10901171 (BioLegend Cat. No. 123131)
AB_11125371 (BioLegend Cat. No. 135219)
AB_2562273 (BioLegend Cat. No. 108739)
AB_11125575 (BioLegend Cat. No. 101239)
AB_2563491 (BioLegend Cat. No. 103255)
AB_11218801 (BioLegend Cat. No. 100749)

AB_312660 (BioLegend Cat. No. 100203)

60 kJ% from fat, 19 kJ% from proteins, and 21 kJ% from carbohydrates

used for dissection purposes

AB_312846 (BioLegend Cat. No. 101903)
AB_313102 (BioLegend Cat. No. 104417)
AB_2290801 (BioLegend Cat. No. 107629)
AB_2563684 (BioLegend Cat. No. 100565)

AB_2076206 (BioLegend Cat. No. 103031)
AB_893561 (BioLegend Cat. No. 108427)

AB_312800 (BioLegend Cat. No. 101301)

viablity stain

jove JOURNAL OF VISUALIZED EXPERIMENTS
1 Alewife Center #200
Cambridge, MA 02140
tel. 617.945.9051
www.jove.com

ARTICLE AND VIDEO LICENSE AGREEMENT

Title of Article: An advanced murine model for myasthenia gravis pseudoparalytica in association with type 2 diabetes

Author(s): Julia Sbierski-Kind, Katharina Schmidt-Bleek, Matthias Stanke, Jonas Kath, Joachim Spranger, Hans-Dieter Volk

Item 1: The Author elects to have the Materials be made available (as described at http://www.jove.com/publish) via:

☐ Standard Access ☒ Open Access

Item 2: Please select one of the following items:

☒ The Author is **NOT** a United States government employee.

☐ The Author is a United States government employee and the Materials were prepared in the course of his or her duties as a United States government employee.

☐ The Author is a United States government employee but the Materials were NOT prepared in the course of his or her duties as a United States government employee.

ARTICLE AND VIDEO LICENSE AGREEMENT

1. **Defined Terms.** As used in this Article and Video License Agreement, the following terms shall have the following meanings: "**Agreement**" means this Article and Video License Agreement; "**Article**" means the article specified on the last page of this Agreement, including any associated materials such as texts, figures, tables, artwork, abstracts, or summaries contained therein; "**Author**" means the author who is a signatory to this Agreement; "**Collective Work**" means a work, such as a periodical issue, anthology or encyclopedia, in which the Materials in their entirety in unmodified form, along with a number of other contributions, constituting separate and independent works in themselves, are assembled into a collective whole; "**CRC License**" means the Creative Commons Attribution-Non Commercial-No Derivs 3.0 Unported Agreement, the terms and conditions of which can be found at: http://creativecommons.org/licenses/by-nc-nd/3.0/legalcode; "**Derivative Work**" means a work based upon the Materials or upon the Materials and other pre-existing works, such as a translation, musical arrangement, dramatization, fictionalization, motion picture version, sound recording, art reproduction, abridgment, condensation, or any other form in which the Materials may be recast, transformed, or adapted; "**Institution**" means the institution, listed on the last page of this Agreement, by which the Author was employed at the time of the creation of the Materials; "**JoVE**" means MyJove Corporation, a Massachusetts corporation and the publisher of The Journal of Visualized Experiments; "**Materials**" means the Article and / or the Video; "**Parties**" means the Author and JoVE; "**Video**" means any video(s) made by the Author, alone or in conjunction with any other parties, or by JoVE or its affiliates or agents, individually or in collaboration with the Author or any other parties, incorporating all or any portion of the Article, and in which the Author may or may not appear.

2. **Background.** The Author, who is the author of the Article, in order to ensure the dissemination and protection of the Article, desires to have the JoVE publish the Article and create and transmit videos based on the Article. In furtherance of such goals, the Parties desire to memorialize in this Agreement the respective rights of each Party in and to the Article and the Video.

3. **Grant of Rights in Article.** In consideration of JoVE agreeing to publish the Article, the Author hereby grants to JoVE, subject to **Sections 4** and **7** below, the exclusive, royalty-free, perpetual (for the full term of copyright in the Article, including any extensions thereto) license (a) to publish, reproduce, distribute, display and store the Article in all forms, formats and media whether now known or hereafter developed (including without limitation in print, digital and electronic form) throughout the world, (b) to translate the Article into other languages, create adaptations, summaries or extracts of the Article or other Derivative Works (including, without limitation, the Video) or Collective Works based on all or any portion of the Article and exercise all of the rights set forth in (a) above in such translations, adaptations, summaries, extracts, Derivative Works or Collective Works and(c) to license others to do any or all of the above. The foregoing rights may be exercised in all media and formats, whether now known or hereafter devised, and include the right to make such modifications as are technically necessary to exercise the rights in other media and formats. If the "Open Access" box has been checked in **Item 1** above, JoVE and the Author hereby grant to the public all such rights in the Article as provided in, but subject to all limitations and requirements set forth in, the CRC License.

jove JOURNAL OF VISUALIZED EXPERIMENTS
1 Alewife Center #200
Cambridge, MA 02140
tel. 617.945.9051
www.jove.com

ARTICLE AND VIDEO LICENSE AGREEMENT

4. **Retention of Rights in Article.** Notwithstanding the exclusive license granted to JoVE in **Section 3** above, the Author shall, with respect to the Article, retain the non-exclusive right to use all or part of the Article for the non-commercial purpose of giving lectures, presentations or teaching classes, and to post a copy of the Article on the Institution's website or the Author's personal website, in each case provided that a link to the Article on the JoVE website is provided and notice of JoVE's copyright in the Article is included. All non-copyright intellectual property rights in and to the Article, such as patent rights, shall remain with the Author.

5. **Grant of Rights in Video – Standard Access.** This **Section 5** applies if the "Standard Access" box has been checked in **Item 1** above or if no box has been checked in **Item 1** above. In consideration of JoVE agreeing to produce, display or otherwise assist with the Video, the Author hereby acknowledges and agrees that, Subject to **Section 7** below, JoVE is and shall be the sole and exclusive owner of all rights of any nature, including, without limitation, all copyrights, in and to the Video. To the extent that, by law, the Author is deemed, now or at any time in the future, to have any rights of any nature in or to the Video, the Author hereby disclaims all such rights and transfers all such rights to JoVE.

6. **Grant of Rights in Video – Open Access.** This **Section 6** applies only if the "Open Access" box has been checked in **Item 1** above. In consideration of JoVE agreeing to produce, display or otherwise assist with the Video, the Author hereby grants to JoVE, subject to **Section 7** below, the exclusive, royalty-free, perpetual (for the full term of copyright in the Article, including any extensions thereto) license (a) to publish, reproduce, distribute, display and store the Video in all forms, formats and media whether now known or hereafter developed (including without limitation in print, digital and electronic form) throughout the world, (b) to translate the Video into other languages, create adaptations, summaries or extracts of the Video or other Derivative Works or Collective Works based on all or any portion of the Video and exercise all of the rights set forth in (a) above in such translations, adaptations, summaries, extracts, Derivative Works or Collective Works and (c) to license others to do any or all of the above. The foregoing rights may be exercised in all media and formats, whether now known or hereafter devised, and include the right to make such modifications as are technically necessary to exercise the rights in other media and formats. For any Video to which this **Section 6** is applicable, JoVE and the Author hereby grant to the public all such rights in the Video as provided in, but subject to all limitations and requirements set forth in, the CRC License.

7. **Government Employees.** If the Author is a United States government employee and the Article was prepared in the course of his or her duties as a United States government employee, as indicated in **Item 2** above, and any of the licenses or grants granted by the Author hereunder exceed the scope of the 17 U.S.C. 403, then the rights granted hereunder shall be limited to the maximum rights permitted under such statute. In such case, all provisions contained herein that are not in conflict with such statute shall remain in full force and effect, and all provisions contained herein that do so conflict shall be deemed to be amended so as to provide to JoVE the maximum rights permissible within such statute.

8. **Protection of the Work.** The Author(s) authorize JoVE to take steps in the Author(s) name and on their behalf if JoVE believes some third party could be infringing or might infringe the copyright of either the Author's Article and/or Video.

9. **Likeness, Privacy, Personality.** The Author hereby grants JoVE the right to use the Author's name, voice, likeness, picture, photograph, image, biography and performance in any way, commercial or otherwise, in connection with the Materials and the sale, promotion and distribution thereof. The Author hereby waives any and all rights he or she may have, relating to his or her appearance in the Video or otherwise relating to the Materials, under all applicable privacy, likeness, personality or similar laws.

10. **Author Warranties.** The Author represents and warrants that the Article is original, that it has not been published, that the copyright interest is owned by the Author (or, if more than one author is listed at the beginning of this Agreement, by such authors collectively) and has not been assigned, licensed, or otherwise transferred to any other party. The Author represents and warrants that the author(s) listed at the top of this Agreement are the only authors of the Materials. If more than one author is listed at the top of this Agreement and if any such author has not entered into a separate Article and Video License Agreement with JoVE relating to the Materials, the Author represents and warrants that the Author has been authorized by each of the other such authors to execute this Agreement on his or her behalf and to bind him or her with respect to the terms of this Agreement as if each of them had been a party hereto as an Author. The Author warrants that the use, reproduction, distribution, public or private performance or display, and/or modification of all or any portion of the Materials does not and will not violate, infringe and/or misappropriate the patent, trademark, intellectual property or other rights of any third party. The Author represents and warrants that it has and will continue to comply with all government, institutional and other regulations, including, without limitation all institutional, laboratory, hospital, ethical, human and animal treatment, privacy, and all other rules, regulations, laws, procedures or guidelines, applicable to the Materials, and that all research involving human and animal subjects has been approved by the Author's relevant institutional review board.

11. **JoVE Discretion.** If the Author requests the assistance of JoVE in producing the Video in the Author's facility, the Author shall ensure that the presence of JoVE employees, agents or independent contractors is in accordance with the relevant regulations of the Author's institution. If more than one author is listed at the beginning of this Agreement, JoVE may, in its sole

1 Alewife Center #200
Cambridge, MA 02140
tel. 617.945.9051
www.jove.com

ARTICLE AND VIDEO LICENSE AGREEMENT

discretion, elect not take any action with respect to the Article until such time as it has received complete, executed Article and Video License Agreements from each such author. JoVE reserves the right, in its absolute and sole discretion and without giving any reason therefore, to accept or decline any work submitted to JoVE. JoVE and its employees, agents and independent contractors shall have full, unfettered access to the facilities of the Author or of the Author's institution as necessary to make the Video, whether actually published or not. JoVE has sole discretion as to the method of making and publishing the Materials, including, without limitation, to all decisions regarding editing, lighting, filming, timing of publication, if any, length, quality, content and the like.

12. **Indemnification.** The Author agrees to indemnify JoVE and/or its successors and assigns from and against any and all claims, costs, and expenses, including attorney's fees, arising out of any breach of any warranty or other representations contained herein. The Author further agrees to indemnify and hold harmless JoVE from and against any and all claims, costs, and expenses, including attorney's fees, resulting from the breach by the Author of any representation or warranty contained herein or from allegations or instances of violation of intellectual property rights, damage to the Author's or the Author's institution's facilities, fraud, libel, defamation, research, equipment, experiments, property damage, personal injury, violations of institutional, laboratory, hospital, ethical, human and animal treatment, privacy or other rules, regulations, laws, procedures or guidelines, liabilities and other losses or damages related in any way to the submission of work to JoVE, making of videos by JoVE, or publication in JoVE or elsewhere by JoVE. The Author shall be responsible for, and shall hold JoVE harmless from, damages caused by lack of sterilization, lack of cleanliness or by contamination due to the making of a video by JoVE its employees, agents or independent contractors. All sterilization, cleanliness or decontamination procedures shall be solely the responsibility of the Author and shall be undertaken at the Author's expense. All indemnifications provided herein shall include JoVE's attorney's fees and costs related to said losses or damages. Such indemnification and holding harmless shall include such losses or damages incurred by, or in connection with, acts or omissions of JoVE, its employees, agents or independent contractors.

13. **Fees.** To cover the cost incurred for publication, JoVE must receive payment before production and publication of the Materials. Payment is due in 21 days of invoice. Should the Materials not be published due to an editorial or production decision, these funds will be returned to the Author. Withdrawal by the Author of any submitted Materials after final peer review approval will result in a US$1,200 fee to cover pre-production expenses incurred by JoVE. If payment is not received by the completion of filming, production and publication of the Materials will be suspended until payment is received.

14. **Transfer, Governing Law.** This Agreement may be assigned by JoVE and shall inure to the benefits of any of JoVE's successors and assignees. This Agreement shall be governed and construed by the internal laws of the Commonwealth of Massachusetts without giving effect to any conflict of law provision thereunder. This Agreement may be executed in counterparts, each of which shall be deemed an original, but all of which together shall be deemed to me one and the same agreement. A signed copy of this Agreement delivered by facsimile, e-mail or other means of electronic transmission shall be deemed to have the same legal effect as delivery of an original signed copy of this Agreement.

A signed copy of this document must be sent with all new submissions. Only one Agreement is required per submission.

CORRESPONDING AUTHOR

Name:	Julia Sbierski-Kind
Department:	Department of Endocrinology and Metabolism, Charité Universitätsmedizin Berlin
Institution:	Corporate member of Freie Universität Berlin und Humboldt-Universität Berlin – Charité
Title:	Dr. med.
Signature:	
Date:	29/11/2018

Please submit a **signed** and **dated** copy of this license by one of the following three methods:

1. Upload an electronic version on the JoVE submission site
2. Fax the document to +1.866.381.2236
3. Mail the document to JoVE / Attn: JoVE Editorial / 1 Alewife Center #200 / Cambridge, MA 02140

Dear Dr. D´Souza,
Please find attached the resubmission of our manuscript JoVE59470 "An advanced murine model for nonalcoholic steatohepatitis in association with type 2 diabetes". Thank you for forwarding the referees report. We also thank you and the referees for the time and effort that they invested into the review of our manuscript, and for their helpful comments and suggestions. Below, we respond to the points raised by the editor and referees. We hope that the work is now ready for publication in JoVE.
Sincerely yours,
Julia Sbierski-Kind

Response to the editorial report
We thank the editor for careful reading of our manuscript and thoughtful comments. Below we reply to the editorial 'suggestions for improvement':

(a) We proofread the manuscript and corrected spelling and grammatical errors.
(b) We made sure that all text in the protocol section is written in the imperative voice and added the text in 1.6 as a note.
(c) We added more details to different steps in the protocol section.
(d) We adjusted the numbering in the protocol section, ensured that all steps are lined up at the left margin, and had a one-line space between each protocol step.
(e) We highlighted the protocol steps to be featured in the video.
(f) We edited the discussion section and complemented comments on future applications and significance with respect to existing methods.
(g) We split Figure 1 into two figures and renumbered the figures.
(h) We changed color-coding in Table 1 and 2.
(i) We defined error bars and black arrowhead in Figure 3.
(j) We used the JoVE EndNote style file in the reference section.
(k) We replaced commercial sounding language and removed the trademark symbols from the table of materials.
(l) We revised the table of materials and listed materials in alphabetical order.

Response to the reviewers report
We thank the reviewers for the thoughtful and thorough review and for detailed comments and suggestions. Below we reply to the reviewers comments.

Reviewer #1:
(a) The referee asked about blood checks performed in mice to identify pathogens. For both animal facilities (housing environmentally exposed and SPF mice) health monitoring was performed in accordance with FELASA recommendations every six months. Please find attached the appropriate health monitoring documents. In our recent publication (see Ref. [13] of the revised manuscript) further differences between both the HFD SPF and HFD exposed mice were described.
(b) The referee suggested commenting on the role of the gut microbiota regarding the different phenotypes of the wildtype mice under different environmental conditions. We

agree with the referee that this is an interesting question. In our recent publication, (see Ref. [13] of the revised manuscript) we already mentioned this issue in the discussion section. Recently, it has been demonstrated that gut barrier function, e.g., intestinal permeability and alterations in intestinal levels of secondary bile acids, depend on housing conditions (see Ref. [21] of the revised manuscript). Therefore, the question whether gut colonization plays a causal role in adipose tissue and liver inflammation arises and is being addressed in another work of our group (in preparation). We added a comment about the role of microbiota in the discussion section, but further details would be beyond the scope of the methodological focus of JoVE.

(c) The referee asked about deeper reasons for not using Fluorescence Minus One (FMO) controls that can help identify gating boundaries. To cut a long story short, we did not use FMO controls in this specific experiment due to pragmatic reasons. Immune cells in murine adipose tissue are limited, so that we decided not to use them for FMO controls. Moreover, we could rely on a relatively high antigen expression in almost all antibodies. Our data could be properly compensated and the gating was clear (except for the CD44 antibody, which could indeed benefit from FMO controls). Of course, we used actual negative controls and single-stain controls to compare our data to in every single experiment.

(d) We thank the referee for bringing up this important question. As mentioned in our previous publication (see Ref. [13] of the revised manuscript) , we were able to describe significant hepatic T cell alterations after 7 weeks of HFD feeding under non-SPF conditions and NASH-like pathology after 15 weeks of HFD feeding. The mechanisms underlying NASH are largely unknown. However, in this context, we point out previous work, that showed that the activation of hepatic $CD8^+$ T cells and NKT cells cause liver steatosis via interactions with hepatocytes via secreted LIGHT[1].

(e) We replaced “reproducible” for “solid” or “robust”.

Reviewer #2:

(a) The referee challenged us to comment on the feasibility of our experimental setup. We are fully aware of the difficulties of non-SPF housing, but we are convinced that the administrative difficulties are fully outweighed by the benefits of environmentally exposed mice. These are valuable for investigating aspects of the hygiene hypothesis and immune functions in order to find treatments for autoimmune diseases or other diseases that involve the immune system. Experiments with SPF mice are still needed as they are inbred and genetically homogenous, but different works already showed, that the development of a human adult-like immune system is compromised in SPF mice (see Ref. [12, 13, 14] of the revised manuscript), which would make it difficult to translate treatment strategies from bench to bedside. With respect to the first mentioned concern (open doors in animal facility), we had separated animal facilities with SPF and dirty mice and suggest that other research institutions should consider this, too. However, we agree with the referee that gloves could be worn by the experimentalist and have changed the text in the method section accordingly. In another, yet unpublished, subsequent experiment with non-SPF mice, we could verify the significant increase of effector memory $CD8^+$ T cells by using non-irradiated food, bedding from pig and daily handling without air shower, mask and hairnet. Thus, to our experience, bedding from mammalian animals (not necessarily sheep) is required for appropriate environmental exposure. Concerning the co-housing of sheep, we have changed the text in the method section,

too. We thank the referee for raising these important concerns and added some points mentioned above to the discussion section.

(b) The referee asked us to specify the housing conditions of non-SPF mice. As mentioned in our previous publication, mice were housed in SPF conditions or transferred to the "dirty" animal facility at the age of 4 weeks and, thus, were not exposed to non-SPF conditions prenatally. We first investigated the immune cell composition of non-SPF mice after 7 weeks of HFD feeding. At this time point, the HFD SPF and HFD non-SPF groups already differed significantly and showed an increase of 20% of effector memory $CD8^+$ T cells of $CD8^+$ T cells as described in our previous publication (see Ref. [13] of the revised manuscript, Figure 3A). This explanation was missing in our discussion and we have added it accordingly. We thank the referee for the thoughtful comment.

(c) The referee challenged us to clarify the metabolic differences between HFD SPF and HFD non-SPF animals. As suggested, we added a summary of our results, already published (see Ref. [13] of the revised manuscript) in the results section of the manuscript.

(d) The referee asked us to comment on the liver histology of non-SPF HFD mice in Figure 2B (now Figure 3B). Unfortunately, we made a mistake here as the liver sections were from 15 weeks fed HFD mice as described in our previous publication (we did not check liver sections from 7 weeks fed HFD mice) and, actually, the Figure is adapted from Figure 7G in our previous publication (see Ref. [13] of the revised manuscript). We apologize for any confusion and corrected the mistake.

(e) The referee suggested commenting on the role of microbial diversity related to immunological and metabolic alterations and we thank the referee for bringing up this important question, too. As described in answer (b) to Reviewer #1 we already addressed the question of gut colonization and subsequent obesity risk in another work, which is in preparation. We therefore added a comment about the role of microbiota in the discussion section.

(f) The referee challenged us to comment on the development of liver steatosis of non-SPF mice dependent on housing conditions. As described in our previous publication (see Ref. [13] of the revised manuscript), hematoxylin/eosin staining of liver sections of mice on HFD for 15 weeks of HFD feeding revealed severe steatosis in exposed mice while only some SPF mice displayed a mild fat accumulation in the liver. Blinded NASH scoring of liver histology confirmed that 8/8 AE mice on 15 weeks HFD displayed a strong NASH phenotype (score > 3–5), whereas NASH was not observed in the majority of SPF mice (5/8, score < 1). The remaining liver sections were categorized as displaying only a mild form of NASH (3/8, score =3). Furthermore, CD3 staining confirmed lobular inflammation in HFD AE mice, whereas Sirius Red staining revealed mild pericellular fibrosis in those mice (see Ref. [13] of the revised manuscript). Unfortunately, we did not have time and resources to perform any transfer experiments and did not change housing conditions after the beginning of the experiment, but thank the referee for raising this interesting point. Beura et al. could show that co-housing pet store mice changes the immune system of SPF laboratory mice (see Ref. [12] of the revised manuscript), but to our knowledge we were the first ones to investigate the influence of environmental conditions on the development of liver steatosis.

(g) The referee asked us to comment on the normalization method of our flow cytometry data and on optimization guidelines for collagenase production. First, we did not normalize the flow cytometry data in our experiments, but each experimental day we included mice from each experimental group to eliminate effects due to day-to-day variation (temperature, incubation time e.g.). This explanation was missing in our

discussion and we have added it accordingly and eliminated the term “normalization” to avoid confusion. Second, our protocol aims to be reproducible, when immune cell isolation is performed in liver or visceral adipose tissue in wildtype C57Bl/6J mice. However, when immune cell isolation is performed in other tissues from different mammalian species, the protocol needs to be adapted relating to collagenase type, digestion times and dissection methods. To address this issue, we adjusted the paragraph in the discussion section.

We would like to thank you for the helpful comments and suggestions. We have taken all recommendations into consideration, and hope that the revised manuscript will be found suitable for publication. We very much appreciate the opportunity to improve our manuscript and have uploaded a substantially revised version in which all changes are indicated.

---

1 Wolf, Monika J. *et al.* Metabolic Activation of Intrahepatic CD8⁺ T Cells and NKT Cells Causes Nonalcoholic Steatohepatitis and Liver Cancer via Cross-Talk with Hepatocytes. *Cancer Cell.* **26** (4), 549-564, doi:10.1016/j.ccell.2014.09.003, (2014).